Hindawi
Journal of Chemistry
Volume 2020, Article ID 8747639, 10 pages
https://doi.org/10.1155/2020/8747639

Research Article

Synthesis and Characterization of Lyophilized Chitosan-Based Hydrogels Cross-Linked with Benzaldehyde for Controlled Drug Release

Fouad Damiri, Yahya Bachra, Chaimaa Bounacir, Asmae Laaraibi, and Mohammed Berrada

University Hassan II of Casablanca, Faculty of Sciences Ben M'Sick, Department of Chemistry, Laboratory of Biomolecules and Organic Synthesis (BIOSYNTHO), Casablanca, Morocco

Correspondence should be addressed to Fouad Damiri; fouad.damiri-etu@etu.univh2c.ma

Received 16 December 2019; Revised 30 March 2020; Accepted 4 May 2020; Published 18 May 2020

Guest Editor: Long Bai

In this study, chitosan-based hydrogels were produced by incorporating three drugs with a different solubility into a polymer matrix. The lyophilized chitosan salt was prepared using an innovative and less-expensive synthetic process by the freeze-drying technique. Firstly, the three drugs (caffeine, ascorbic acid, and 5-fluorouracil (5-FU)) were selected as model drugs to test the in vitro release behavior of the hydrogel. The drugs were solubilized in chitosan salt, lyophilized, and cross-linked with benzaldehyde involving the formation of a Schiff base with (–C=N-) linkage to produce a physical hydrogel. Subsequently, the physicochemical properties of N-benzyl chitosan and lyophilized chitosan salt were evaluated by Fourier-transform infrared (FTIR) spectra, scanning electron microscopy (SEM), and thermogravimetric analysis (TGA). The intrinsic viscosity of the conventional chitosan was determined by the Mark–Houwink–Sakurada equation. Moreover, the kinetics of hydrogel swelling and drug release were studied by the UV-visible method at physiological conditions (pH = 7.4 at 37°C). The results show that lyophilized N-benzyl chitosan had a maximum swelling ratio of 720 ± 2% by immersion in phosphate-buffered saline solutions (PBS) (pH = 7.4 at 37°C). In vitro drug releases were evaluated in PBS, and the obtained results show that the maximum drug release after 24 h was 42% for caffeine, 99% for 5-FU, and 94% for ascorbic acid. Then, to optimize the cumulative release of caffeine, Tween 20 was added and 98% as a release percentage was obtained. The drug-loading results were investigated with the Korsmeyer–Peppas kinetic model and applied to determine the drug release mechanism.

1. Introduction

Drug delivery systems (DDS) are pharmaceutical formulations used to transport therapeutic drugs and the bioactive molecules in the body as needed to safely achieve the desired therapeutic effect. Such systems are usually designed to improve aqueous solubility and chemical stability of active agents, increase pharmacological activity, and reduce side effects [1, 2]. The goal of any drug delivery system has an important role to play in the administration of vaccines, drugs, and diagnostic agents [3]. Systems based on biodegradable polymer and a cross-linking agent may be particularly advantageous for the controlled release of drugs [4].

Lyophilized chitosan salt with a well-defined degree of deacetylation (DDA) gives spongious materials (chitosan sponges) that are useful biomaterials, which can be easily loaded with drugs such as antibiotics, anti-inflammatory drugs, and growth-promoting proteins. The drug release takes place over time as long as the chitosan swells [5–7]. The easy loading of drugs is attributable in part to chitosan's cationic nature, which promotes swelling and electrostatic interactions between the polymer and aqueous proteins and drugs that have a net negative charge. The cationic nature also provides mucoadhesive properties for adhering chitosan to mucosal and other tissues that can be used to help retain it at intended sites of drug delivery. Chitosan is commonly

dissolved in dilute organic acid (e.g., acetic acid and lactic acid) because these solvents are commonly used to dissolve the chitosan before lyophilization, and the resulting sponges will contain acidic salts in the form of the chitosan amino ($-NH^{3+}$) group and the carboxylic (COO^{-}) group of the organic acid. These salts will easily hydrate and redissolve with a reformation of organic acid in aqueous solutions [8]. Therefore, the lyophilization process is a generally simple and efficient technique to prepare chitosan sponges in which the solvent acetic acid exists in the frozen chitosan solution. The chitosan solution was neutralized with NaOH aqueous solution to remove the excess acid molecules before the lyophilization.

Hydrogels are three-dimensional networks composed of hydrophilic polymers cross-linked through covalent bonds or held together via physical intermolecular interactions [9, 10]. Over the past few decades, methods for administering drugs via hydrogels have gained increasing attention, as regulating the rate of drug release with a controlled release; the mechanism offers numerous advantages over conventional dosage regimens [11, 12]. The use of polysaccharide-based hydrogels as a drug delivery carrier in biomedical and pharmaceutical applications has contributed to resolving relatively complicated biocompatibility problems owing to their nontoxicity, biodegradability [13], and biocompatibility systems [14–18]. Many approaches have been reported for the preparation of chitosan-based hydrogels [19, 20], including those based on chemical as well as physical cross-linking methods. Although physical methods have the advantage of a cross-link structure without the use of cross-linking agents, they exhibit a disadvantage in the lack of precise control over the quality of chemical properties of the obtained gels. On the other hand, the physical cross-linking of the chitosan hydrogels can easily be carried out using benzaldehyde as a hydrophobic cross-linking agent [21–24]. However, this cross-linking agent generally has associated toxicities and a small amount of free residual cross-linking agent may remain if the resulting hydrogels are not well washed with an aqueous solution during synthesis, which will be potentially harmful to human health [25].

Important features of hydrogels are the controlled release of therapeutic products and their ability to encapsulate drugs in their inflated network of water that make them commonly used biomaterials [26]. However, hydrogels as drug delivery systems have been limited to the transport of drugs with good water solubility, and the major problem usually encountered is the incorporation of poorly soluble drugs [27]. In this study, we have chosen three drugs with different solubility: caffeine, 5-FU, and ascorbic acid.

Caffeine (1,3,7-trimethylxanthine) is an alkaloid of the xanthine group [28, 29]. Unfortunately, caffeine (Figure 1) is sparingly soluble in water (20 g/L at room temperature and 660 g/L at boiling point) and is in the form of white, soft, odorless powder with a melting point of 235°C–238°C. Natural sources of caffeine include different varieties of coffee beans, tea leaves, guarana seeds, mate leaves, kola nut seeds, and cocoa beans [30].

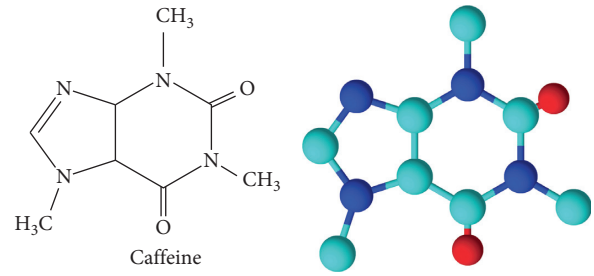

Figure 1: Chemical structure of caffeine.

5-FU (Figure 2) is an anticancer drug with broad activity against solid tumors with a solubility of nearly 11.1 g/L in the water at 22°C. It belongs to the class of cytotoxic anticancer drugs that have side effects, which has inhibited its use despite its effectiveness in interfering or killing fast-growing cancer cells [31, 32].

Ascorbic acid (vitamin C) is a water-soluble vitamin (300 g/l at 20°C) and is also a necessary nutrient for maintaining the physiological balance of the process in humans and some animals. However, the main source of ascorbic acid are citrus fruits such as orange [33]. A wide variety of other foods also contain sufficient amounts of vitamin C (Figure 3), such as pineapple, sweet pepper, broccoli, kale, cauliflower, black currant, and rosehip [34].

Polysorbate 20 or Tween 20 (Figure 4) is a stable nonionic and nontoxic surfactant widely used in a variety of scientific, pharmaceutical, food, and cosmetic applications [35, 36]. Tween 20 is a polyoxyethylene derivative of sorbitan monolaurate, distinguished from the other Tween molecules by the length of the fatty acid ester moiety [35].

Therefore, the purpose of this study was to prepare an N-benzyl chitosan hydrogel incorporating three drugs of different solubility. Two strategies used for enhancing the bioavailability of drugs were (1) using the N-benzyl chitosan matrix consisting of lyophilized chitosan salt and (2) using Tween 20 as a surfactant to improve the solubility of the poorly soluble drug in the physiological medium, pH = 7.4 and $T = 37$°C, in order to optimize the release of the drug [37].

Our research aims are to develop a smart drug delivery system (DDS), having the property to dissolve very fast in the PBS medium to get an injectable solution. The biomaterial should stay liquid at room temperature and become solid at 37°C after the formation of hydrogel into the body. In the literature, only a few articles reported the N-benzyl chitosan hydrogel synthesis. However, we are probably the first scientific team that reports the preparation of biomaterials as drug delivery systems based on spongious chitosan completely water-soluble that was grafted with benzaldehyde and forms a hydrogel by physical cross-linking. In this research, the N-benzyl chitosan hydrogel was used to deliver soluble, sparingly soluble, or insoluble drugs. The observed drug delivery problem with insoluble ones was solved by adding a surfactant. As an example, Tween 20, a nonionic surfactant, was used in PBS to obtain the desired profile release of the active ingredients.

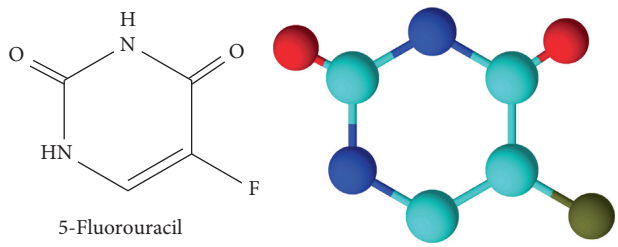

Figure 2: Chemical structure of 5-fluorouracil.

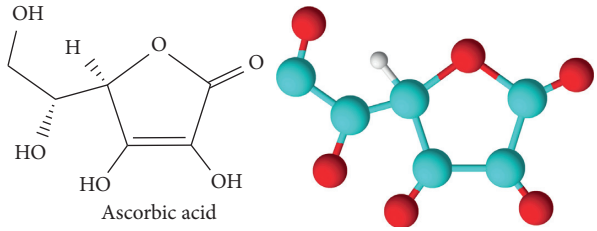

Figure 3: Chemical structure of ascorbic acid.

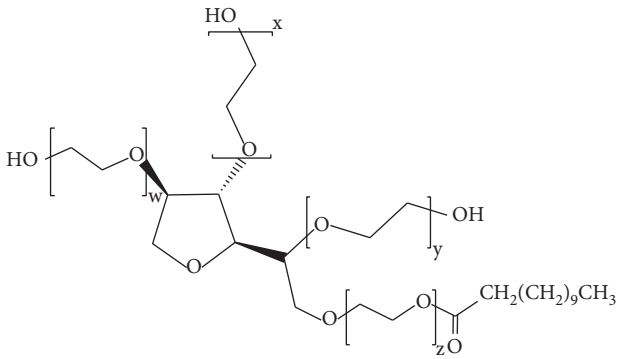

Figure 4: Chemical structure of Tween 20.

2. Materials and Methods

2.1. Materials. Chitosan (DDA = 94%), caffeine (Sigma-Aldrich), 5-fluorouracil (Sigma-Aldrich), ascorbic acid (Fluka), benzaldehyde (Loba Chemie), Tween 20 (Sigma-Aldrich), acetic acid (Sigma-Aldrich), ethanol (AnalaR-Normapur), sodium bicarbonate (Sigma-Aldrich), and PBS (phosphate-buffered saline, pH = 7.4) were used.

2.2. Intrinsic Viscosity Measurements. The viscosity average molecular weight (M_v) of the prepared chitosans was calculated by the Mark–Houwink equation:

$$[\eta] = KM^{\alpha}, \quad (1)$$

where $K = 6.59 \times 10^{-5}$ dl/g and $\alpha = 0.88$ at 30°C [38]. The viscosity measurements were performed in 0.2 M acetic acid and 0.1 M sodium acetate using an Ubbelohde viscometer at 30°C with a capillary diameter of 0.63 mm.

2.3. Fabrication of the Lyophilized Chitosan Salt. 1 g of pure chitosan was dissolved in acetic acid (1% w/w), the mixture was magnetically stirred at ambient temperature overnight, and then NaOH 1 N was added carefully to the chitosan solution at $T = 0$°C to neutralize it to pH = 6.2 avoiding the chitosan precipitation. The solution (Figure 5) was frozen overnight at −40°C and then lyophilized (by Alpha 1–2 LD_{plus}) at −50°C for 24 hours in a freeze dryer [39].

Chitosan was soluble in acetic acid solution. Therefore, the group (CH_3COO^-) is the anion, and (NH_3^+--chitosan) is the counter ion.

2.4. Synthesis of Chitosan-Based Hydrogels Cross-Linked with Benzaldehyde. To prepare water-soluble chitosan that can dissolve quickly, we have used the lyophilization process. 1 g of lyophilized chitosan salt was dissolved in 60 ml of distilled water at pH = 5.9. The solution was then diluted with 30 mL of ethanol and stirred at $T = 0$°C for 1 hour. 100 mg of solubilized drug was added into the chitosan. Benzaldehyde (0.960 g) was dissolved in 10 ml ethanol under stirring for 1 hour at 0°C, before adding it to the chitosan solution. The reaction mixture was stirred at 0°C for 2 hours. The pH of the solution was adjusted to 7.4 with 6% (w/v) $NaHCO_3$. At 37°C, a transparent gel was obtained (Figures 6 and 7). The hydrogel was washed with ethanol and filtered to remove benzaldehyde traces.

Lyophilized chitosan was grafted by benzaldehyde moieties involving the formation of a Schiff base with (–C=N-) linkage. The grafted chitosan was cross-linked by hydrophobic interactions generated by the aromatic moieties in the backbones. The grafting is a chemical reaction, but cross-linking is a physical interaction.

2.5. In Vitro Release Studies. Samples of 500 mg of the chitosan/benzaldehyde solution with or without drug were placed into circular-shaped molds (diameter 8 mm) and allowed to gel in an incubator at 37°C for 2 h. The circular-shaped gels were removed, placed into histology cassettes, and suspended in 1000 mL of isotonic phosphate-buffered saline (PBS, pH 7.4) containing 3% Tween 20. Tween 20 was included in the release medium to increase the solubility of caffeine.

2.6. Scanning Electron Microscopy (SEM). The morphology of the N-benzyl chitosan hydrogel and lyophilized chitosan salt was examined with a scanning electron microscopy SEM (MiniSEM Hirox SH-4000).

2.7. Equilibrium Swelling Study. The hydrogel samples were lyophilized at −80°C and immersed in PBS (pH = 7.4) at 37°C for a maximum time of 24 h, during which the gel reached an equilibrium state of swelling. Swollen samples were removed at different time intervals 15 min, 1 h, and 24 h. The following formula was used to calculate the water sorption capacity. The results obtained were calculated using equation (2) as the mean ± standard deviation ($n = 3$) according to the reported study [40]:

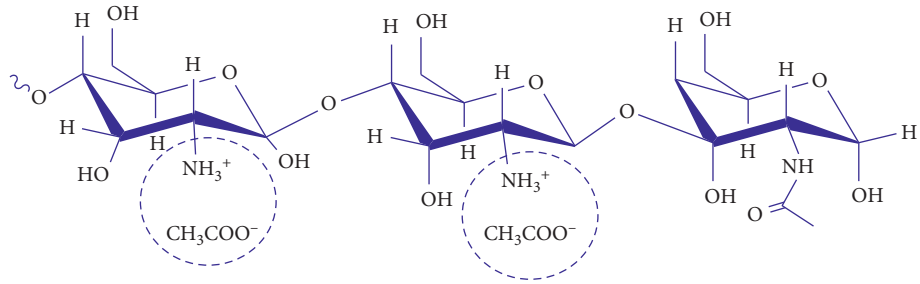

Figure 5: Structure of lyophilized chitosan salt.

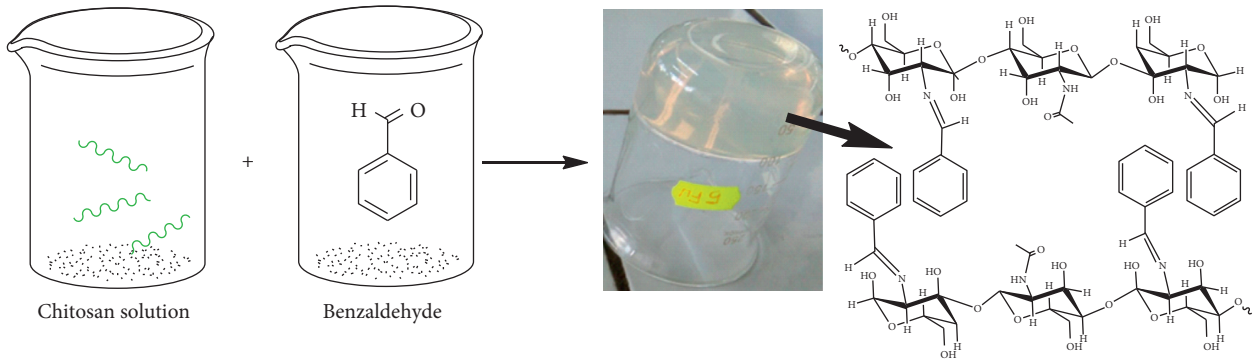

Figure 6: Chitosan-based hydrogel cross-linked with benzaldehyde.

$$\text{Swelling ratio\%} = \frac{(W_1 - W_0) \times 100}{W_0}, \quad (2)$$

where W_0 is the weight of the dry hydrogel after lyophilization and W_1 is the weight of the swollen hydrogel.

2.8. Fourier-Transform Infrared (FTIR) Spectra. Fourier-transform infrared spectra (FTIR) of the lyophilized chitosan salt and the hydrogel were collected using a spectrum 400 PerkinElmer operating in the range of 400–4000 cm^{-1}.

2.9. Thermogravimetric Analysis (TGA). The thermal properties of lyophilized chitosan salt and chitosan were studied by thermogravimetric analysis (TGA). The samples were placed in the balance system and heated from 40°C to 600°C at a heating rate of 10°C/min using a TA Instruments TGA (Q_{500}) device.

2.10. In Vitro Drug Release from the Hydrogels. In vitro drug release studies were carried out by placing the drug-loaded hydrogels in 1000 mL of the PBS-releasing medium at 37°C and taking out 2 mL aliquots at particular time intervals.

The drug amount released from the hydrogel was determined spectrophotometrically at the drug λ_{max} in a Shimadzu UV-Vis spectrophotometer (UV-1800). The withdrawn aliquots were replaced with equal volumes of phosphate buffer solution and Tween 20 to simulate physiological conditions. The concentration of the drug released was estimated from the calibration plot of the drug. The release data were expressed as the mean value of three independent experiments, and the standard deviations are also presented as error bars.

The concentrations of the three drugs were analyzed with a UV-Vis spectrophotometer. Drug-free hydrogels were treated similarly, and solutions were analyzed for drugs, but no signals were obtained from these samples. Standards of each drug were also added to blank samples to determine whether the presence of the polymer affected the outcome of analysis; no anomalous effects were observed. The λ_{max} values for 5-FU, caffeine, and ascorbic acid were, respectively, 266 nm, 273 nm, and 265 nm.

The concentration of the drug in the PBS solution was obtained from the calibration curve, and the amount of drug released at time t (M_t) was calculated by accumulating the total drug release up to that time.

The fractional drug release M_t/M_0 could then be calculated using the following equation:

$$\text{\%cumulative release} = \frac{M_t}{M_0} \times 100, \quad (3)$$

where "M_t" is the amount of drug released at the time (t) and "M_0" is the maximal amount of the drug released at the maximum interval.

2.11. Statistical Analysis. The experimental data from all the studies were analyzed, and the results are presented as mean ± standard deviation. Error bars represent the standard deviation ($n = 3$).

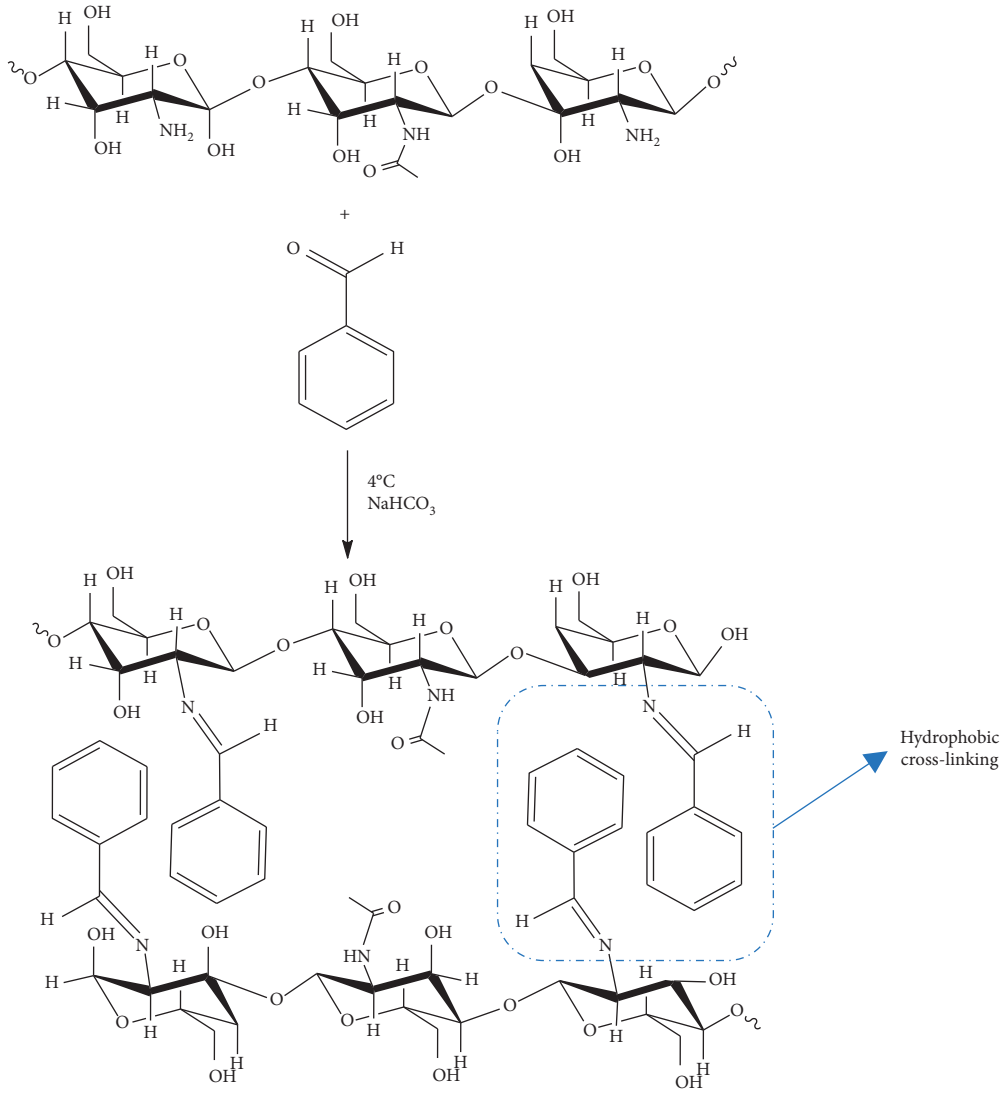

Figure 7: Schematic representation of the formation process of the physical hydrogel.

3. Results and Discussion

3.1. Intrinsic Viscosity Measurements. The molecular weight of the chitosan was determined using an Ubbelohde viscometer.

Viscosity average molecular weight (M_w) was calculated from the following equation:

$$\log[\eta] = \mathrm{Log}K + \alpha \mathrm{Log}M_w, \tag{4}$$

where $[\eta]$ is the intrinsic viscosity of the chitosan and K and α are the constants for the given solute-solvent system and temperature. For chitosan, they are influenced by the degree of deacetylation, pH, and ionic strength of the solvent. As to the chitosan with a DDA value of 94%, the constants $K = 6.59 \times 10^{-5}$ dl/g and $\alpha = 0.88$ at 30°C. The viscosity average molecular weight of the chitosan (Figure 8) was therefore calculated as follows:

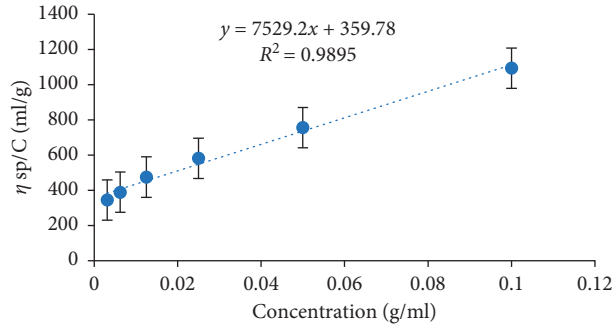

Figure 8: Relation between ηsp/C and concentration of pure chitosan solution.

$$\log(359.78) = \log\left(6.59 \times 10^{-3}\right) + 0.88\log(M_w),$$
$$M_w = 241.546\,KDa. \tag{5}$$

3.2. Thermogravimetric Analysis (TGA). The thermogravimetric analysis (TGA) of conventional chitosan and lyophilized chitosan salt is shown in Figure 9. The conventional chitosan (Figure 9 a) showed the first thermal loss at 92°C with a mass loss of 11% assigned to the water adsorbed and/or weakly hydrogen bonded to chitosan. The second thermal loss reached a maximum at 397°C with a mass loss of 46%. It corresponded to the thermal decomposition of the pyranose ring with the rupture of the glycosidic linkages between the glucosamine and N-acetylglucosamine rings on chitosan and release of volatile products. It was also observed a mass loss of 18% and a residual mass of 25% at 600°C [41]. Moreover, in the TGA curve of lyophilized chitosan salt (Figure 9 b), two distinct decomposition temperatures were observed. The first step of weight loss from 38% was between 110°C and 195°C; however, the second thermal loss 29.79% was between 244°C and 515°C. The freeze-dried chitosan sponge is less thermostable compared to the conventional chitosan obtained by precipitation in ethanol. The results indicated that spongious chitosan degraded quickly than conventional chitosan [8].

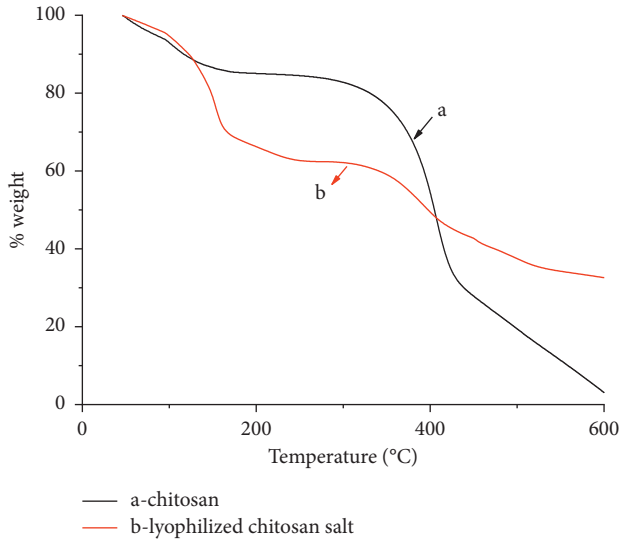

Figure 9: Thermogravimetric analysis (TGA) of lyophilized chitosan salt and conventional chitosan.

3.3. Fourier-Transform Infrared (FTIR) Spectra. The FTIR spectrum of chitosan was recorded in the region of 4000–400 cm^{-1} and is shown in Figure 10. The spectrum of conventional chitosan (Figure 10) shows a wide band around 3450 cm^{-1} corresponding to amine N–H symmetrical vibration and H bonded O–H group. The peak observed between 3400 and 3800 cm^{-1} correspond to a combination of the band O-H, NH_2, and intramolecular hydrogen bonding. The peaks at 2920 and 2320 cm^{-1} are assigned to the symmetric and asymmetric $-CH_2$ vibrations of the carbohydrate ring. The absorption peaks are at 1650 cm^{-1} (C=O in amide group, amide I vibration), 1545 cm^{-1} ($-NH_2$ bending of amide II), and 1390 cm^{-1} (N–H stretching or C–N bond stretching vibrations, amide III vibration). The peak observed at 1050 cm^{-1} has a contribution to the symmetric stretching of C–O–C groups. The absorption peaks in the range 900–1200 cm^{-1} are due to the antisymmetric C–O stretching of the saccharide structure of chitosan [42]. Figure 10 shows the FTIR spectra of lyophilized chitosan salt obtained from solutions of chitosan (acetic acid). Firstly, the purely electrostatic nature of the interaction between chitosan and acetic acid is confirmed. FTIR spectra of lyophilized chitosan salt exhibited an absorption peak of carboxylate salt ($-COO^-$) of the acetic side chain that was bound to an amino group ($-NH^{3+}$) of chitosan at 1590 cm^{-1} via electrostatic interaction. The second observation exhibited an absorption broad peak of free ions (OH^- and H^+) in the range of 2700 cm^{-1}–3700 cm^{-1}. Thus, from the FTIR profile, the successful fabrication of the sponges has been confirmed [8]. In Figure 11, the spectrum of (N-BzCS) formation occurred via the corresponding Schiff base "imine" band which appeared as a sharp peak at 1632 cm^{-1}, confirming the covalent bonding of N-benzyl chitosan, also mentioned in these studies [21, 41, 43, 44].

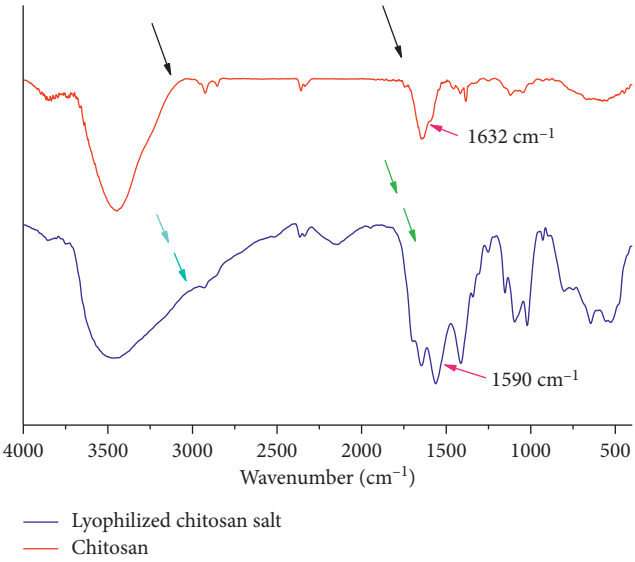

Figure 10: FTIR spectra of conventional chitosan and lyophilized chitosan salt.

3.4. Scanning Electron Microscopy (SEM) Analysis. The surface morphologies of lyophilized chitosan salt and N-BzCS hydrogels are presented in Figure 12. The SEM images of uncross-linked lyophilized chitosan salt showed irregular and random fibrous structures (Figure 12 (a) and (b)) compared to cross-linked chitosan that showed a microporous structure (Figure 12 (c) and (d)) when the images were magnified. A methodology for the precise determination of the microporous volume and BET surface area based on the volume difference in nitrogen physisorption isotherms at 77 K and 298 K is under development.

3.5. Equilibrium Swelling Study. The hydrogel swelling process was studied and represented as a function of time (Figure 13). The pure chitosan is soluble in the physiological medium (pH = 7 and 4°C to 37°C) and could not form a

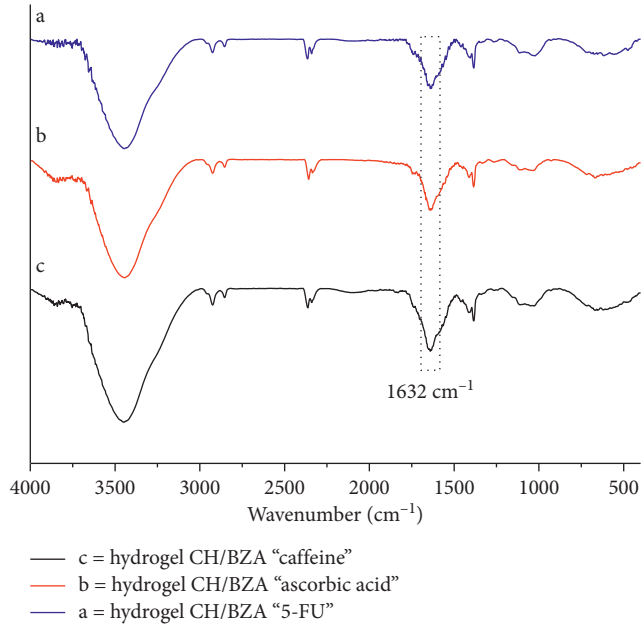

Figure 11: FTIR spectra of drug loaded into a physical hydrogel.

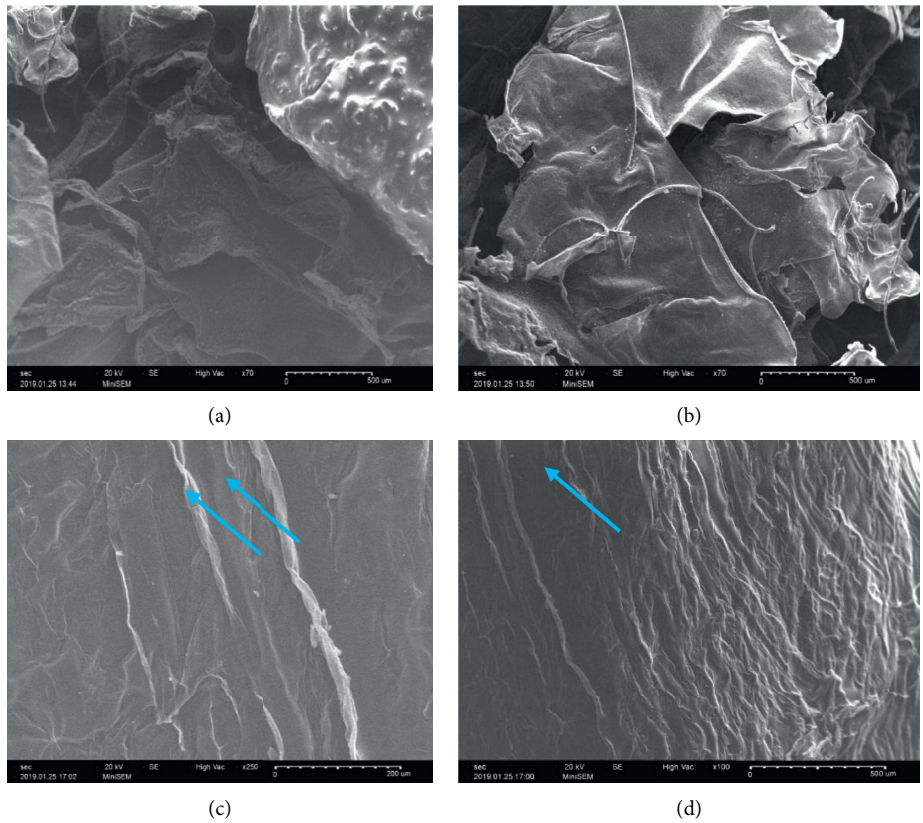

Figure 12: Representative cross-sectional SEM images of lyophilized chitosan salt ((a) and (b)) and chitosan-based hydrogel ((c) and (d)).

hydrogel without a cross-linking reaction. The hydrogel swelling was obtained by immersion in a buffer solution (pH = 7.4 at 37°C). All lyophilized hydrogel samples absorb water quickly. The rate of swelling gradually increased over time and reached equilibrium in about 24 hours.

The hydrogel swelling behavior has been studied and, as shown in Figure 13, the hydrogel has water sorption properties. Hydrogels absorb about 720 times more water than their weight. The percentage of swelling increased with soaking time, until it reached a steady state after about 24

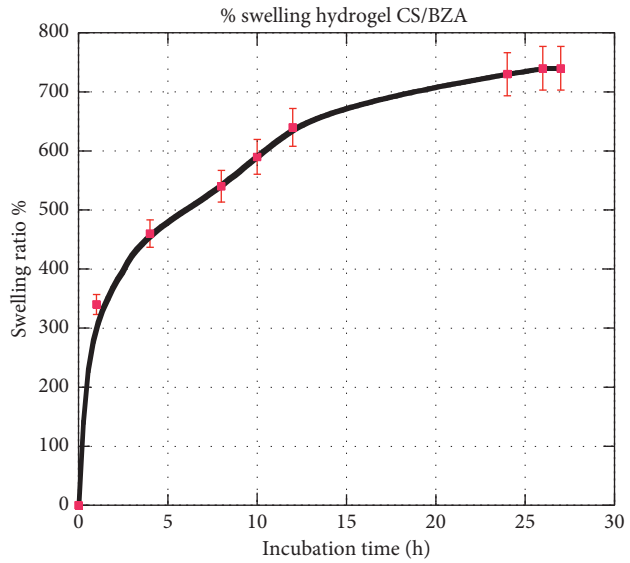

Figure 13: % swelling degree (SD).

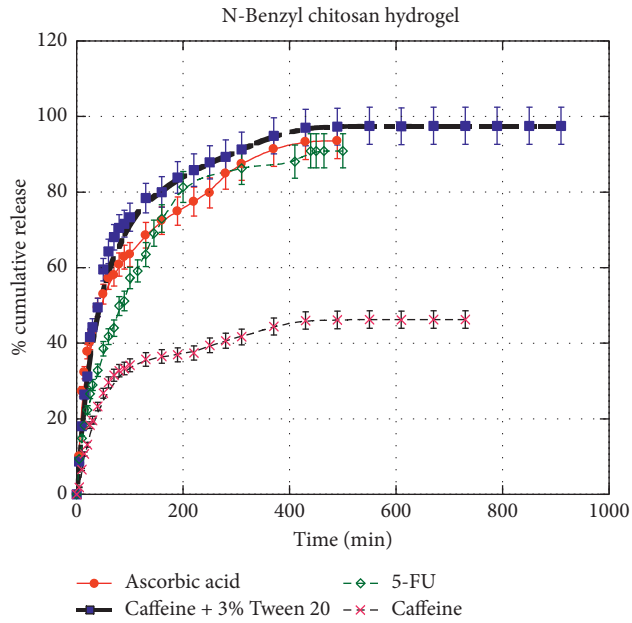

Figure 14: In vitro drug release from hydrogels at 37°C in PBS at pH 7.4.

hours. The amount of water in a hydrogel and its "character" of free water or bound water will determine the absorption and diffusion of solutes through the hydrogel. They can exist as smaller pores in the network. The average pore size, pore size distribution, and pore interconnections are important factors in a hydrogel matrix that are often difficult to quantify.

Figure 13 shows the trend in the swelling degree which is depending on the cross-linking ratio of the hydrogel and the swelling rate of the chitosan hydrogel. In Figure 13, the rate of inflation is increased proportionally over time. It can be concluded that the higher the degree of cross-linking, the lower the amount of water trapped inside the polymer and a low swelling rate [45, 46]. Hence, the absorption and swelling capacity of chitosan hydrogels depend on the degree of cross-linking [47].

3.6. In Vitro Drug Release from the Hydrogels. The 5-fluorouracil, caffeine, and ascorbic acid have been taken as model drugs to investigate the loading efficiency and release profile as a function of time. In this study, 100 mg of drug was loaded into the hydrogel. The drug encapsulation efficiency of the hydrogel was found to be 42% for caffeine, 99% for 5-FU, and 98% of ascorbic acid as measured by the UV-Vis spectroscopic method. The in vitro cumulative drug release studies were carried out in a physiological media PBS (pH = 7.4 at 37°C). Error bars represent the standard deviation ($n = 3$). 5-Fluorouracil (5-FU) was highly water soluble under the conditions of controlled release compared to caffeine which was only moderately water soluble. The release of 5-FU from different biomaterials, developed by Berrada et al. [31], showed a similar release pattern compared to the results obtained in this contribution. The drug could be released from the hydrogel in a sustained period. The initial drug-loading amount had a great effect on the drug release profile. With lower initial drug-loading amounts, the drug released faster and reached a higher cumulative release rate compared to higher initial drug-loading hydrogel as reported by Berrada et al. [31, 48–50]. The addition of Tween 20 in PBS improved the solubility of the drug to release into the physiological medium. The in vitro cumulative release of caffeine in the Tween 20/PBS media was reported as displayed in (Figure 14). The cumulative release profile was checked for 24 h at a fixed time interval [51, 52]. On the other hand, 98% of caffeine was released from the hydrogel in 3% Tween 20/PBS. This result suggests that a release of the three drugs (caffeine, 5-FU, and ascorbic acid) was sensitive to solubility. Initially, there was a burst release (around first 50 min) due to the quantity of the drug on the surface of the hydrogel which allowed it to be released quickly, followed by a slow release after 2 hours. The small burst release of caffeine was due to physically adsorbed caffeine on the outer shell of the polymer layer and not the result of the hydrogel biodegradation. The imine bond was quite stable, and its hydrolysis kinetic was slow [51, 52]. However, about 10% of the drug remains trapped in the hydrogel after 6 hours, which could be due to the interaction between the hydrogel matrix and the drugs.

There are several factors (degree of deacetylation (DDA), molecular weight, drug's charge, etc.) influencing the drug release from the polymer matrix than solubility. However, in this study, we kept constant the molecular weight and the degree of deacetylation (DDA).

The in vitro release behavior of 5-FU from our hydrogel showed an initial burst release of 32% of loaded 5-FU occurred in the first one hour, followed by releasing of 90% in 8 hours. However, the in vitro release behavior of 5-FU from a biodegradable copolymer PEG-PCL-PEG (PECE) triblock hydrogel (25 wt%) studied by Wang et al. [53] showed that 5-FU was released from the 5-FU hydrogel in a sustained period. In the PECE hydrogel containing 0.5 mg 5-FU, an

initial burst release of 26.2% of loaded 5-FU occurred in the first one hour, followed by releasing of 82.9% in one day.

4. Conclusion

This paper has been focused on the preparation of N-benzyl chitosan hydrogels as drug delivery systems (DDS). We have reported the synthesis of the N-benzyl chitosan biomaterial based on chitosan that was grafted with benzaldehyde. From 4°C to room temperature, this material is liquid but becomes quickly a hydrogel at 37°C. The physical cross-linking was obtained via the hydrophobic interactions between aromatic moieties in the backbone. Overall, the results showed several advantages of this polymer as a drug delivery system. Caffeine, 5-FU, and ascorbic acid were used as model drugs showing interesting release behavior. The excellent properties of the developed DDS demonstrated that an in situ targeted therapy can be achieved. However, its efficacy also needs to be further proved and confirmed by a larger number of future studies. The biocompatibility and toxicity tests are under study for our N-benzyl chitosan hydrogel to check its potential use in biomedical applications.

This work offers an efficient and practical way to prepare smart-responsive hydrogels from chitosan. These smart hydrogels can have wide applications in the fields of pharmaceutical, agriculture, and food.

Data Availability

The data used to support the findings of this study are available from the corresponding author upon request.

Conflicts of Interest

The authors declare that they have no conflicts of interest.

References

[1] K. Park, "Controlled drug delivery systems: past forward and future back," *Journal of Controlled Release*, vol. 190, pp. 3–8, 2014.

[2] C. Li, J. Wang, Y. Wang et al., "Recent progress in drug delivery," *Acta Pharmaceutica Sinica B*, vol. 9, 2019.

[3] X. Zhao, P. Li, B. Guo, and P. X. Ma, "Antibacterial and conductive injectable hydrogels based on quaternized chitosan-graft-polyaniline/oxidized dextran for tissue engineering," *Acta Biomaterialia*, vol. 26, pp. 236–248, 2015.

[4] B. Guo, J. Qu, X. Zhao, and M. Zhang, "Degradable conductive self-healing hydrogels based on dextran-graft-tetraaniline and N-carboxyethyl chitosan as injectable carriers for myoblast cell therapy and muscle regeneration," *Acta Biomaterialia*, vol. 84, pp. 180–193, 2019.

[5] J. Berretta, J. D. Bumgardner, and J. A. Jennings, "Lyophilized chitosan sponges," *Chitosan Based Biomater*, Elsevier, vol. 1, pp. 239–253, Amsterdam, Netherlands, 2017.

[6] L. Illum, N. F. Farraj, and S. S. Davis, "Chitosan as a novel nasal delivery system for peptide drugs," *Pharmaceutical Research*, vol. 11, no. 8, pp. 1186–1189, 1994.

[7] S. A. Agnihotri, N. N. Mallikarjuna, and T. M. Aminabhavi, "Recent advances on chitosan-based micro- and nanoparticles in drug delivery," *Journal of Controlled Release*, vol. 100, no. 1, pp. 5–28, 2004.

[8] Y. Kotchamon and P. Thawatchai, "Role of aluminum monostearate on heat treated-chitosan sponges properties," *Journal of Metals, Materials and Minerals*, vol. 22, pp. 75–82, 2012.

[9] J. Qu, X. Zhao, Y. Liang, Y. Xu, P. X. Ma, and B. Guo, "Degradable conductive injectable hydrogels as novel antibacterial, anti-oxidant wound dressings for wound healing," *Chemical Engineering Journal*, vol. 362, pp. 548–560, 2019.

[10] X. Qi, T. Su, M. Zhang et al., "Macroporous hydrogel scaffolds with tunable physicochemical properties for tissue engineering constructed using renewable polysaccharides," *ACS Applied Materials & Interfaces*, vol. 12, no. 11, pp. 13256–13264, 2020.

[11] X. Zhao, H. Wu, B. Guo, R. Dong, Y. Qiu, and P. X. Ma, "Antibacterial anti-oxidant electroactive injectable hydrogel as self-healing wound dressing with hemostasis and adhesiveness for cutaneous wound healing," *Biomaterials*, vol. 122, pp. 34–47, 2017.

[12] J. Qu, X. Zhao, Y. Liang, T. Zhang, P. X. Ma, and B. Guo, "Antibacterial adhesive injectable hydrogels with rapid self-healing, extensibility and compressibility as wound dressing for joints skin wound healing," *Biomaterials*, vol. 183, pp. 185–199, 2018.

[13] X. Hu, Y. Wang, L. Zhang, M. Xu, W. Dong, and J. Zhang, "Redox/pH dual stimuli-responsive degradable Salecan-g-SS-poly(IA-co-HEMA) hydrogel for release of doxorubicin," *Carbohydrate Polymers*, vol. 155, pp. 242–251, 2017.

[14] H. Kono and T. Teshirogi, "Cyclodextrin-grafted chitosan hydrogels for controlled drug delivery," *International Journal of Biological Macromolecules*, vol. 72, pp. 299–308, 2015.

[15] C. Alvarez-Lorenzo, B. Blanco-Fernandez, A. M. Puga, and A. Concheiro, "Crosslinked ionic polysaccharides for stimuli-sensitive drug delivery," *Advanced Drug Delivery Reviews*, vol. 65, no. 9, pp. 1148–1171, 2013.

[16] N. Bhattarai, J. Gunn, and M. Zhang, "Chitosan-based hydrogels for controlled, localized drug delivery," *Advanced Drug Delivery Reviews*, vol. 62, no. 1, pp. 83–99, 2010.

[17] I. Charhouf, A. Benaamara, A. Abourriche, and M. Berrada, "Characterization of Chitosan and fabrication of Chitosan hydrogels matrices for biomedical applications," *MATEC Web of Conferences*, vol. 5, p. 04030, 2013.

[18] X. Hu, Y. Wang, L. Zhang, and M. Xu, "Formation of self-assembled polyelectrolyte complex hydrogel derived from salecan and chitosan for sustained release of Vitamin C," *Carbohydrate Polymers*, vol. 234, p. 115920, 2020.

[19] L. Weng, N. Rostambeigi, N. D. Zantek et al., "An in situ forming biodegradable hydrogel-based embolic agent for interventional therapies," *Acta Biomaterialia*, vol. 9, no. 9, pp. 8182–8191, 2013.

[20] N. Samadi, M. Sabzi, and M. Babaahmadi, "Self-healing and tough hydrogels with physically cross-linked triple networks based on Agar/PVA/Graphene," *International Journal of Biological Macromolecules*, vol. 107, pp. 2291–2297, 2018.

[21] E. I. Rabea, M. E. I. Badawy, W. Steurbaut, and C. V. Stevens, "In vitro assessment of N-(benzyl)chitosan derivatives against some plant pathogenic bacteria and fungi," *European Polymer Journal*, vol. 45, no. 1, pp. 237–245, 2009.

[22] C. Yu, X. Kecen, and Q. Xiaosai, "Grafting modification of chitosan," *Biopolymer Grafting: Synthesis and Properties*, Elsevier, Amsterdam, Netherlands, pp. 295–364, 2018.

[23] V. L. Triana-Guzmán, Y. Ruiz-Cruz, E. L. Romero-Peñaloza, H. F. Zuluaga-Corrales, and M. N. Chaur-Valencia, "New chitosan-imine derivatives: from green chemistry to removal

of heavy metals from water," *Revista Facultad de Ingeniería Universidad de Antioquia*, no. 89, pp. 34–43, 2018.

[24] X. Wang, P. Xu, Z. Yao et al., "Preparation of antimicrobial hyaluronic acid/quaternized chitosan hydrogels for the promotion of seawater-immersion wound healing," *Frontiers in Bioengineering and Biotechnology*, vol. 7, 2019.

[25] F. Ullah, M. B. H. Othman, F. Javed, Z. Ahmad, and H. M. Akil, "Classification, processing and application of hydrogels: a review," *Materials Science and Engineering: C*, vol. 57, pp. 414–433, 2015.

[26] X. Qi, W. Wei, J. Shen, and W. Dong, "Salecan polysaccharide-based hydrogels and their applications: a review," *Journal of Materials Chemistry B*, vol. 7, no. 16, pp. 2577–2587, 2019.

[27] S. J. Buwalda, T. Vermonden, and W. E. Hennink, "Hydrogels for therapeutic delivery: current developments and future directions," *Biomacromolecules*, vol. 18, no. 2, pp. 316–330, 2017.

[28] J. Tello, M. Viguera, and L. Calvo, "Extraction of caffeine from Robusta coffee (Coffea canephora var. Robusta) husks using supercritical carbon dioxide," *The Journal of Supercritical Fluids*, vol. 59, pp. 53–60, 2011.

[29] J. M. Kalmar and E. Cafarelli, "Effects of caffeine on neuromuscular function," *Journal of Applied Physiology*, vol. 87, no. 2, pp. 801–808, 1999.

[30] H. Ashihara and A. Crozier, "Caffeine: a well known but little mentioned compound in plant science," *Trends in Plant Science*, vol. 6, no. 9, pp. 407–413, 2001.

[31] M. Berrada, Z. Yang, and S. Lehnert, "Tumor treatment by sustained intratumoral release of 5-fluorouracil: effects of drug alone and in combined treatments," *International Journal of Radiation Oncology∗Biology∗Physics*, vol. 54, no. 5, pp. 1550–1557, 2002.

[32] A. Tutkun, S. İnanlı, O. Caymaz, E. Ayanoğlu, and D. Duman, "Cardiotoxicity of 5-flourouracil: two case reports," *Auris Nasus Larynx*, vol. 28, no. 2, pp. 193–196, 2001.

[33] S. J. Devaki and R. L. Raveendran, "Vitamin C: sources, functions, sensing and analysis," *Vitamin C,* InTech, London, UK, 2017.

[34] M. Moser and O. Chun, "Vitamin C and heart health: a review based on findings from epidemiologic studies," *International Journal of Molecular Sciences*, vol. 17, no. 8, p. 1328, 2016.

[35] A. Masotti, P. Vicennati, A. Alisi et al., "Novel Tween 20 derivatives enable the formation of efficient pH-sensitive drug delivery vehicles for human hepatoblastoma," *Bioorganic & Medicinal Chemistry Letters*, vol. 20, no. 10, pp. 3021–3025, 2010.

[36] B. A. Kerwin, "Polysorbates 20 and 80 used in the formulation of protein biotherapeutics: structure and degradation pathways," *Journal of Pharmaceutical Sciences*, vol. 97, no. 8, pp. 2924–2935, 2008.

[37] Y. C. Ching, T. M. S. U. Gunathilake, C. H. Chuah, K. Y. Ching, R. Singh, and N.-S. Liou, "Curcumin/Tween 20-incorporated cellulose nanoparticles with enhanced curcumin solubility for nano-drug delivery: characterization and in vitro evaluation," *Cellulose*, vol. 26, no. 9, pp. 5467–5481, 2019.

[38] M. R. Kasaai, J. Arul, and G. R. Charlet, "Intrinsic viscosity-molecular weight relationship for chitosan," *Journal of Polymer Science Part B: Polymer Physics*, vol. 38, no. 19, pp. 2591–2598, 2000.

[39] M. Wang, Y. Ma, Y. Sun et al., "Hierarchical porous chitosan sponges as robust and recyclable adsorbents for anionic dye adsorption," *Scientific Reports*, vol. 7, p. 18054, 2017.

[40] S. Anbazhagan and K. P. Thangavelu, "Application of tetracycline hydrochloride loaded-fungal chitosan and Aloe vera extract based composite sponges for wound dressing," *Journal of Advanced Research*, vol. 14, pp. 63–71, 2018.

[41] W. Sajomsang, S. Tantayanon, V. Tangpasuthadol, M. Thatte, and W. H. Daly, "Synthesis and characterization of N-aryl chitosan derivatives," *International Journal of Biological Macromolecules*, vol. 43, no. 2, pp. 79–87, 2008.

[42] A. Laaraibi, F. Moughaoui, F. Damiri et al., "Chitosan-clay based (CS-NaBNT) biodegradable nanocomposite films for potential utility in food and environment," *Chitin-Chitosan-Myriad Functionalities in Science and Technology*, InTech, London, UK, 2018.

[43] G. Crini, G. Torri, M. Guerrini, M. Morcellet, M. Weltrowski, and B. Martel, "NMR characterization of N-benzyl sulfonated derivatives of chitosan," *Carbohydrate Polymers*, vol. 33, no. 2-3, pp. 145–151, 1997.

[44] M. E. I. Badawy, E. I. Rabea, T. M. Rogge et al., "Synthesis and fungicidal activity of NewN,O-acyl chitosan derivatives," *Biomacromolecules*, vol. 5, no. 2, pp. 589–595, 2004.

[45] M.-M. Iftime, S. Morariu, and L. Marin, "Salicyl-imine-chitosan hydrogels: supramolecular architecturing as a cross-linking method toward multifunctional hydrogels," *Carbohydrate Polymers*, vol. 165, pp. 39–50, 2017.

[46] H. S. Samanta and S. K. Ray, "Controlled release of tinidazole and theophylline from chitosan based composite hydrogels," *Carbohydrate Polymers*, vol. 106, pp. 109–120, 2014.

[47] Z. Yue, Y. Che, Z. Jin et al., "A facile method to fabricate thermo- and pH-sensitive hydrogels with good mechanical performance based on poly(ethylene glycol) methyl ether methacrylate and acrylic acid as a potential drug carriers," *Journal of Biomaterials Science, Polymer Edition*, vol. 30, no. 15, pp. 1375–1398, 2019.

[48] M. Berrada, A. Serreqi, F. Dabbarh, A. Owusu, A. Gupta, and S. Lehnert, "A novel non-toxic camptothecin formulation for cancer chemotherapy," *Biomaterials*, vol. 26, no. 14, pp. 2115–2120, 2005.

[49] E. Ruel-Gariépy, M. Shive, B. Bichara et al., "A thermosensitive chitosan-based hydrogel for the local delivery of paclitaxel," *European Journal of Pharmaceutics and Biopharmaceutics*, vol. 57, pp. 53–63, 2004.

[50] M. Berrada, Z. Yang, and S. M. Lehnert, "Sensitization to radiation from an implanted 125I source by sustained intratumoral release of chemotherapeutic drugs," *Radiation Research*, vol. 162, no. 1, pp. 64–70, 2004.

[51] R. C. Mundargi, V. Rangaswamy, and T. M. Aminabhavi, "A novel method to prepare 5-fluorouracil, an anti-cancer drug, loaded microspheres from poly(N-vinyl caprolactam-co-acrylamide) and, controlled release studies," *Designed Monomers and Polymers*, vol. 13, no. 4, pp. 325–336, 2010.

[52] V. Ramezani, M. Honarvar, M. Seyedabadi, A. Karimollah, A. M. Ranjbar, and M. Hashemi, "Formulation and optimization of transfer some containing minoxidil and caffeine," *Journal of Drug Delivery Science and Technology*, vol. 44, pp. 129–135, 2018.

[53] X. Wang, W. Yang, and J. Yang, "Extramammary Paget's disease with the appearance of a nodule: a case report," *BMC Cancer*, vol. 10, no. 1, 2010.